

## Discovery of an Isolated Compact Object at High Galactic Latitude

R. E. Rutledge<sup>1</sup>, D. B. Fox<sup>2</sup>, & A. H. Shevchuk<sup>2</sup>

### ABSTRACT

We report discovery of a compact object at high Galactic latitude. The object was initially identified as a *ROSAT* All-Sky Survey Bright Source Catalog X-ray source, 1RXS J141256.0+792204, statistically likely to possess a high X-ray to optical flux ratio. Further observations using *Swift*, Gemini-North, and the *Chandra* X-ray Observatory refined the source position and confirmed the absence of any optical counterpart to an X-ray to optical flux ratio of  $F_X(0.1\text{--}2.4\text{ keV})/F_V > 8700$  ( $3\sigma$ ). Interpretation of 1RXS J141256.0+792204—which we have dubbed Calvera – as a typical X-ray-dim isolated neutron star would place it at  $z \approx 5.1$  kpc above the Galactic disk – in the Galactic halo – implying that it either has an extreme space velocity ( $v_z \gtrsim 5100\text{ km s}^{-1}$ ) or has failed to cool according to theoretical predictions. Interpretations as a persistent anomalous X-ray pulsar, or a “compact central object” present conflicts with these classes’ typical properties. We conclude the properties of Calvera are most consistent with those of a nearby (80 to 260 pc) radio pulsar, similar to the radio millisecond pulsars of 47 Tuc, with further observations required to confirm this classification. If it is a millisecond pulsar, it has an X-ray flux equal to the X-ray brightest millisecond pulsar (and so is tied for highest flux); is the closest northern hemisphere millisecond pulsar; and is potentially the closest known millisecond pulsar in the sky, making it an interesting target for X-ray-study, a radio pulsar timing array, and *LIGO*.

*Subject headings:* X-rays — neutron stars — X-ray sources: individual: 1RXS J141256.0+792204

---

<sup>1</sup>Department of Physics, McGill University, 3600 rue University, Montreal, QC, H3A 2T8, Canada; rutledge@physics.mcgill.ca

<sup>2</sup>Department of Astronomy & Astrophysics, 525 Davey Laboratory, Pennsylvania State University, University Park, PA 16802, USA; dfox@astro.psu.edu, ahs148@psu.edu

## 1. Introduction

During the past decade, seven isolated neutron stars (INSs), exhibiting no detectable radio pulsar activity, have been discovered in nearby regions of our Galaxy via X-ray surveys. These INSs exhibit thermal emission spectra with peak energies in the far-ultraviolet or soft X-ray, from atmospheres that are thought to be amenable to theoretical modeling (e.g., Lattimer & Prakash 2004; Page & Reddy 2006). As such, they are promising candidates for precision radius measurements via X-ray spectroscopy – measurements that ultimately aim to constrain theories of the nuclear equation of state.

We are currently pursuing a long-term project to identify new isolated neutron stars from within the *ROSAT* All-Sky Survey Bright Source Catalog (BSC; Voges et al. 1999) using short  $\sim 1000$  s observations with NASA’s *Swift* satellite (Gehrels et al. 2004). Although the scientific focus of the *Swift* mission is on gamma-ray burst (GRB) studies, its autonomous pointing capability, rapid one degree per second slewing, and joint X-ray + UV/optical instrumentation make it an excellent platform for such large-scale surveys (Fox 2004), as well as for generic targets of opportunity (TOOs).

We select our targets for *Swift* using statistical techniques of catalog cross-correlation (Rutledge et al. 2003), comparing sources from the BSC to the USNO-A2.0, IRAS point-source, and NVSS catalogs, and selecting sources that are likely, on general grounds, to possess high  $L_X/L_{\text{opt/IR/radio}}$  (see also Rutledge et al. 2000). Our candidate INS sources are then observed with *Swift* on a time-available basis as “fill-in targets,” with a low priority that is guaranteed not to preempt GRB and time-sensitive TOO observations.

Before discussing the results of our survey, we note that the term “isolated neutron star” (INS), although it appears generic, has in fact been adopted to refer exclusively to the seven known non-radio pulsar, non-magnetar, non supernova-remnant associated neutron stars. Since we will be selecting targets on the basis of a high X-ray to optical flux ratio,  $F_X(0.1\text{--}2.4 \text{ keV})/F_V$ , which admits these several types of compact object into our sample, we find it necessary to define a more inclusive term: the “isolated compact object” or ICO. The ICO is an object demonstrated to have a sufficiently high  $F_X(0.1\text{--}2.4 \text{ keV})/F_V$  that its nature as a compact object is assured, with the only remaining question being what type of compact object it is – and an INS being one such possibility.

In this paper we discuss the first ICO (and candidate INS) to be identified from our survey, 1RXS J141256.0+792204. In §2, we present our suite of observations of this source, which demonstrate an X-ray to optical flux ratio  $F_X(0.1\text{--}2.4 \text{ keV})/F_V > 8700$ , sufficient to establish it as a compact object. Given its unique set of properties, we re-christen the source Calvera, and in §3, discuss its properties in relation to known compact object classes. Estab-

lishing a preferred interpretation, while challenging in the absence of further observations, proves to be a useful exercise, casting light on larger questions related to the nature of the known populations of isolated compact objects. Our current state of knowledge and best interpretation of Calvera are then presented in §4.

## 2. Observations & Analysis

We observed the Bright Source Catalog source 1RXS J141256.0+792204 with the *Swift* satellite beginning at 01:25 UT on 25 August 2006. The single observation, extending over two satellite orbits, yielded 1.9 ksec of simultaneous exposure with the satellite’s X-ray Telescope (XRT; Burrows et al. 2003) and Ultraviolet/Optical Telescope (UVOT; Roming et al. 2000) instruments. UVOT observations were taken exclusively through the UVM2 filter, with filter transmission peaking at 220 nm, and XRT observations were in Photon Counting mode. We reduced the data using a custom pipeline derived from official mission data analysis tools (HEASOFT, v6.2) and CIAO v3.4 (Fruscione et al. 2006), with XRT event grades 0–12 accepted for analysis.

The *Swift* XRT data recover the bright X-ray source 1RXS J141256.0+792204, allow an improved estimate of the source position, and provide a broadband X-ray spectrum. The X-ray source position and its statistical uncertainty were derived using `wavdetect`. We extracted 81 source counts from within 30'' of the best position, and 51 background counts from a 3.3' radius circle centered 7.3' from the source position. The expected number of background counts in the source region is  $1.2 \pm 0.2$ , which we neglect in the forgoing analysis.

This X-ray spectrum (Table 1) was fit using the standard products response matrix `swxpc0to12_20010101v008.rmf` and an ancillary response matrix produced using the FTOOLS task `xrtmkarf`, in XSPEC v12.3.0 (Arnaud 1996). The column density ( $N_H$ ) is held fixed at the Galactic value (Dickey & Lockman 1990), because the small number of counts do not permit a strong constraint on  $N_H$ ; also,  $N_H$  is sufficiently low ( $3 \times 10^{20} \text{ cm}^{-2}$ ) that either doubling  $N_H$  or setting  $N_H=0 \text{ cm}^{-2}$  result in an effective temperature ( $kT_{\text{eff}}$ ) within the best fit 90% confidence statistical uncertainty.

We first attempted to bin the spectrum into four spectral bins, corresponding to energy ranges 0.3-1.0, 1.0-2.0, 2.0-5.0 and 5.0-10 keV, which contain 44, 28, 2 and 0 counts, respectively. The number of counts in these bins is so low, that for two such bins, the usual assumption for  $\chi^2$  statistics, that the error bars can be approximated as Gaussian, does not hold; thus, with two spectral bins where this assumption does hold (with number of counts  $>15$ ) and two spectral parameters to be fit, the observed X-ray spectrum has too low

of signal-to-noise ratio to exclude a blackbody spectral model (or any other  $\geq 2$  parameter model). However, we can derive maximum likelihood spectral parameters, and their uncertainties; a statistic which is better for doing so when the number of X-ray counts is low is the Cash statistic (Cash 1979), which we use to derive the maximum likelihood parameter values and their uncertainties.

The INs are all well-described by thermal (blackbody) spectral models. The best-fit blackbody model for Calvera gives  $kT_{\text{eff}}=215\pm 25$  eV, and  $R_{\text{bb}}=7.3^{+2.6}_{-1.7}$  km (d/10 kpc) (uncertainties given are 90% confidence).

Alternatively, the best-fit photon power-law slope is  $2.8\pm 0.3$ ; a thermal bremsstrahlung model has best-fit  $kT_{\text{Brems}} = 0.8^{+0.3}_{-0.2}$  keV, and the best-fit Raymond-Smith plasma has a temperature  $kT_{\text{R-S}} = 1.5^{+0.6}_{-0.3}$  keV.

The simultaneous UVOT observation reveals no 220 nm counterpart to a two-sigma limiting magnitude of 21.6 mags, or  $1.27 \times 10^{-17}$  erg  $\text{cm}^{-2} \text{s}^{-1}$ .

The high X-ray to UV flux ratio established by the *Swift* observations, combined with limits on the brightness of any optical (DSS) or near-infrared (2MASS) counterparts from archival surveys, led us to pursue Director’s Discretionary Time observations with the Gemini telescope. Our subsequent Gemini North + Gemini Multiobject Spectrograph (GMOS-N) observations were taken in queue-observing mode as  $4 \times 600$  s images with mean epoch 14:46 UT on 22 Dec 2006. Data were bias-subtracted, flat-fielded, fringe-subtracted, registered, and combined with cosmic-ray rejection using Gemini pipeline software and official calibration products; the photometric zero-point was derived by reference to ten unsaturated USNO-B1.0 catalog stars in the image. Our resulting image of the region of sky around the source reveals three potential optical counterparts (A–C) with  $g$ -band magnitudes of  $g_1 = 24.80(8)$  mag,  $g_2 = 25.64(10)$  mag, and  $g_3 = 25.86(12)$  mag, respectively, where the uncertainties in the final significant digits are given in parentheses. These sources are at J2000 coordinates  $\alpha_1 = 14 : 12 : 56.64$ ,  $\delta_1 = +79 : 22 : 04.4$ ;  $\alpha_2 = 14 : 12 : 57.76$ ,  $\delta_2 = +79 : 22 : 08.8$ ; and  $\alpha_3 = 14 : 12 : 57.95$ ,  $\delta_3 = +79 : 22 : 00.2$ , respectively, and can be seen in Fig. 1, which shows our final image, smoothed with a PSF-like Gaussian kernel of FWHM  $1.2''$  to reveal faint sources.

In order to eliminate the possibility of associating 1RXS J141256.0+792204 with these faint optical sources, we obtained a 2.1 ksec DDT observation with the *Chandra*/HRC-I (Murray et al. 1998). A wide-field (imaging) observing mode, which has degraded fast-timing capabilities, was selected to include within the field-of-view an unrelated X-ray point source (SWIFT J141055.1+791309;  $\approx 10'$  from Calvera), also detected in our *Swift* XRT observation. We detected 190 counts within  $2''$  of the best-fit position for Calvera, where

only  $0.388 \pm 0.004$  are expected due to background.

Our `wavdetect` analysis reveals just one other faint X-ray source, CXOU J141259.43+791958, at  $2'$  off-axis. This source lies within the field of view (FOV) of our Gemini observations, and can be associated with a bright point-like optical source in this image. It thus offers the opportunity to make a direct registration of the *Chandra* and Gemini observations.

We calculate our best estimates for the *Chandra* positions of Calvera and CXOU J141259.43+791958 using an iterative, weighted-centroiding algorithm that weights photon positions according to a Gaussian approximation of the PSF, which we find to be a superior approach to standard unweighted centroid analyses. Uncertainties in the resulting positions are determined by bootstrap Monte Carlo analysis: in each of 10,000 trials, we resample all detected photons within a large window around the target object, drawing with replacement, and then executing our centroiding algorithm in full, saving all resulting positions. Our quoted 90%-confidence radius corresponds to the minimum-radius circle enclosing 90% of the resulting Monte Carlo positions.

We find a *Chandra* position for CXOU J141259.43+791958 of R.A. 14:12:59.45, Dec. +79:19:58.00 (J2000), with 90%-confidence uncertainty of  $0.48''$ , which is distinctly offset from our Gemini position of R.A. 14:12:59.43, Dec. +79:19:58.95 (J2000). We prefer to quote positions from the Gemini astrometry, which is registered to the USNO-B1.0 catalog astrometry with precision  $0.14''$  precision (RMS), and note that since our final aim is to position Calvera on the Gemini image, any overall error in the Gemini astrometry has no impact in this context. Within  $2''$  of the best-fit position, we find 8 source counts. CXOU J141259.43+791958 was not detected in the SWIFT observation, as its flux ( $5 \times 10^{-14}$  erg cm $^{-2}$  s $^{-1}$ , assuming 1 HRC count =  $1.3 \times 10^{-11}$  erg cm $^{-1}$ , for photon powerlaw slope 2.0 and  $N_H = 3 \times 10^{20}$  cm $^{-2}$ ) was below the detection limit for the SWIFT observation.

The registration of CXOU J141259.43+791958 results in an offset of  $0.04''$  West,  $0.95''$  North ( $\approx 0.95''$  total) to *Chandra* coordinate positions, yielding the position for Calvera that we quote in Table 1: R.A. 14:12:55.885, Dec. +79:22:04.10 (J2000), with a 90%-confidence uncertainty of  $0.57''$  that incorporates the centroiding uncertainty for Calvera as well as, conservatively, the  $0.14''$  precision of the Gemini astrometric mapping. There are 533 USNO-B1.0 objects with  $R > 18.6$  within  $10'$  of CXOU J141259.43+791958; the probability of one lying  $< 0.95''$  from the *Chandra* position is  $1.3 \times 10^{-3}$ , which we regard as sufficient to demonstrate the *Chandra* source is associated with the Gemini source.

Finally, we note that our  $0.95 \pm 0.22$  arcsec offset from the *Chandra* native astrometry is anomalous according to the mission operations team, with  $0.6''$  radial uncertainty at 90%-confidence being the expected performance. However, following our observations the

Chandra X-ray Center reported discovery of a  $0.5''$  systematic offset in ACIS observations taken after December 2006, attributed to an altered spacecraft thermal environment, which may be relevant in this context<sup>1</sup>.

Figure 1 displays the X-ray localization for 1RXS J141256.0+792204 in the context of our Gemini  $g$ -band image. The nearest point source (“A”), southeast of the *Chandra* localization, has  $g = 24.8$  mag and is excluded as a counterpart with  $> 3.8\sigma$  confidence. We therefore detect no  $g$ -band counterpart to a  $3\sigma$  limit of  $g > 26.3$  mag, or  $F_g < 0.11 \mu\text{Jy}$  at  $4750 \text{ \AA}$ . The expected extinction is  $A_g = 0.18$  mag towards the source, as estimated from Galactic extinction maps as well as the source’s X-ray spectrum. As the  $g$  and  $V$ -band zero points are the same, we find an extinction-corrected X-ray to optical flux ratio of  $F_X(0.1\text{--}2.4 \text{ keV})/F_V > 8700$  for 1RXS J141256.0+792204.

A power density spectrum finds no evidence for periodicity at any frequency between  $4.66 \times 10^{-4}$  and 1024 Hz with weak limits on % root-mean-squared variability of  $< 41\%$ , high compared with detected periodicities from known INSs (Durant & van Kerkwijk 2006). The total observed HRC-I average countrate is 52 c/s; the nature of the HRC-I wiring error is such that the absolute timing uncertainty is  $\sim 0.02 \text{ sec}^2$ . Thus, while it is outside the scope of this paper to fully address the sensitivity of observations with degraded timing capabilities to a periodic signal, the  $< 41\%$  r.m.s. variability limit will apply to periodicities in the range  $\sim 0.001\text{--}50$  Hz, but not to higher frequency periodicities.

Comparing the spatial distribution of events in the HRC-I focal plane to the distribution expected for a point source with the spectrum of 1RXS J141256.0+792204, using an 85,000-photon ChaRT simulation (Carter et al. 2003), indicates that the source remains unresolved at sub-arcsecond *Chandra* resolution. Our 90%-confidence upper limits on the fractional contribution from any resolved component are  $< 16\%$  for a resolved component with Gaussian FWHM of 1 arcsec, and  $< 10\%$  for a resolved component with Gaussian FWHM  $\gtrsim 5$  arcsec.

### 3. Discussion

The X-ray to optical flux ratio of 1RXS J141256.0+792204,  $F_X(0.1\text{--}2.4 \text{ keV})/F_V > 8700$ , is comparable to published limits that have accompanied the discovery of several INSs: 1RXS J185635.1–375433 ( $F_X/F_V > 7000$ , Walter et al. 1996), RX J1605.3+3249 ( $F_X/F_V \geq 10^4$ ,

---

<sup>1</sup> Chandra Electronic Bulletin # 60; [http://cxc.harvard.edu/bulletin/bulletin\\_60.html](http://cxc.harvard.edu/bulletin/bulletin_60.html)

<sup>2</sup>A technical description of this error and its effect on the time-tags of individual photons is available at <http://cxc.harvard.edu/cal/Hrc/timing.html>

Motch et al. 1999), 1RXS J130848.6+212708 ( $F_X/F_V > 12000$ , Schwope et al. 1999), and 1RXS J214303.7+065419 ( $F_X/F_V > 10^3$ , Zampieri et al. 2001). In all cases the extreme value of  $F_X/F_V$  was used to exclude all non-compact object source classes. Indeed, all these sources have subsequently been confirmed as INSs, and no counterexamples – sources identified as ICOs on the basis of  $F_X/F_V$  and subsequently demonstrated not to be compact objects – exist in the literature. The fact that high  $F_X/F_V$ , sometimes coupled with detection of X-ray pulsations, is used to identify INSs (Walter et al. 1996; Walter & Matthews 1997; Haberl et al. 1997; Motch et al. 1999; Schwope et al. 1999; Zampieri et al. 2001), and that none has yet been shown to be another class of source, argues for the robustness of this approach. We conclude that 1RXS J141256.0+792204 is a new ICO and candidate INS, for which we adopt the name “Calvera.”

With neither a direct distance measurement nor a proposed association for Calvera, however – and without high signal-to-noise X-ray spectroscopy to confront emission models – our discussion of the physical properties of the source must begin by exploring the range of possible emission models, accepting that both the spectral form and emitting area are largely unconstrained at present. We will therefore discuss each possible model for Calvera in turn: isolated neutron star, magnetar, compact central object, or radio pulsar.

### 3.1. Classifying Calvera

In this section, we consider four possible compact object classifications. In doing so, it will be useful to refer to two figures. In Figures 2 and 3 we compare the X-ray luminosities, thermal blackbody radii ( $R_{\text{bb}}$ ) and effective temperatures ( $kT_{\text{eff}}$ ) for four classes of compact objects – INSs, magnetars, MSPs and CCOs – with Calvera. Here, the luminosities for the CCOs (Pup A, Hui & Becker 2006; G266.1-1.2, Pavlov et al. 2001; Cas A, Pavlov et al. 2000; G330.2+1.0, Park et al. 2006) and INSs (from Haberl 2005 and references therein) are the thermal bolometric luminosities. We use the bolometric thermal luminosities of the MSPs in 47 Tuc (Bogdanov et al. 2006) as indicative of those in the field. Magnetar luminosities (Durant & van Kerkwijk 2006; Munro et al. 2007) are in the 2–10 keV band (bolometric luminosities will be greater).

Before attempting to classify Calvera within the context of these two figures, and their corresponding source populations, we make a general observation. The CCOs, magnetars and INSs are all thought to be thermally powered (i.e., due to core and crustal cooling, including effects of magnetic field decay; Arras et al. 2004). These classes occupy different areas of the ( $kT_{\text{eff}}$ ,  $R_{\text{bb}}$ ) diagram. The youngest objects (CCOs, with the object in Westerlund 1 being the notable exception; Munro et al. 2006) are located in the lower right (high

$kT_{\text{eff}}$ , low  $R_{\text{bb}}$ ), older objects (magnetars) are in the upper right (high  $kT_{\text{eff}}$ , high  $R_{\text{bb}}$ ), and the oldest objects (INSs) are in the upper-left (low  $kT_{\text{eff}}$ , high  $R_{\text{bb}}$ ). This may suggest a population synthesis model in which individual objects evolve with time through the ( $kT_{\text{eff}}$ ,  $R_{\text{bb}}$ ) diagram. Although this is speculative – and we leave detailed consideration to future work – for our present purposes it is sufficient to point out that these three classes of sources, plus the MSPs of 47 Tuc, occupy different areas of the ( $kT_{\text{eff}}$ ,  $R_{\text{bb}}$ ) and ( $R_{\text{bb}}$ ,  $L_X$ ) diagrams. The diagrams are therefore a useful means to compare the properties of Calvera to those of each class of compact object.

In the following sections, we compare Calvera’s properties with the typical source properties of known classes of compact objects which have been identified among field X-ray sources. The alternative is that Calvera has unique properties – for example, an  $R_{\text{bb}}$  or  $L_X$  unlike those of previously identified classes, perhaps due to a different atmospheric composition, magnetic field configuration, or object size, which we call the “It Can Be Any Size” hypothesis (ICBAS). The implication of the ICBAS hypothesis is that no statement about Calvera’s distance (and thus luminosity or  $R_{\text{bb}}$ ) can be made. The ICBAS hypothesis cannot be falsified in the absence of a distance measurement; we therefore do not discuss it further.

### 3.1.1. Isolated Neutron Star

Since the observational approach used to classify Calvera is identical to that of the observationally homogeneous class of INSs – the so-called Magnificent Seven (Haberl 2006) – one might expect that Calvera shares observational properties with this class. As we show in this section, the properties of Calvera diverge from the known INSs.

Despite deep observations of the seven INSs with *Chandra* and *XMM-Newton*, the emergent X-ray spectra of objects in this class are not well understood. The spectrum of the brightest one, 1RXS J185635.1–375433, is accurately described by a blackbody in the X-ray passband (Burwitz et al. 2003), but its optical emission, while also thermal, requires a second blackbody component with a lower temperature and larger emission area (Pons et al. 2002). The only proposed X-ray spectrum which is consistent with both X-ray and optical spectra is composed of an optically thin layer of magnetized hydrogen (Ho et al. 2007). Other INSs also display thermal spectra in the X-ray passband.

Modeling the X-ray spectra of all INSs as thermal blackbodies of identical emission area ( $R_{\text{bb}}=d T_{\text{eff}}^{-2} \sqrt{(\text{B.C.}) F_X/\sigma}$ , where  $d$  is source distance,  $F_X$  is the 0.1–2.4 keV flux, B.C. is the bolometric correction,  $\sigma$  is the Stefan-Boltzman constant), we normalize the INS distances to the parallax distance  $d = 167_{-12}^{+18}$  pc for 1RXS J185635.1–375433 Kaplan et al. 2007, while

noting that this recent result is larger than previous derived distances (Walter & Lattimer 2002; Kaplan et al. 2002). The resulting inferred luminosities and three-dimensional locations of the seven known INSs, and Calvera, are given in Table 2, and displayed in Fig. 4.

While our approach assumes  $R_{\text{bb}}$  is identical for all INSs, this assumption may not be correct: e.g., compare the range of  $R_{\text{bb}}$  values measured for various magnetars (Durant & van Kerkwijk 2006; 2–10 km – a factor of 5). It nonetheless is consistent with the newly-measured parallax distance for the INS RX J0720.4–31225 to the level of accuracy required for the present comparison (parallax distance  $d = 360_{-90}^{+170}$  pc and blackbody distance  $d \approx 500$  pc; Kaplan et al. 2007).

Calculated in this way, all but one previously-known INS have distances from the midplane of the Galactic disk  $|z| < 0.5$  kpc (the exception is 1RXSJ 130848.6+212708,  $z = 1.3$  kpc). Under the same interpretation Calvera’s distance is  $d = 8.4$  kpc from the Sun, and  $z = 5.1$  kpc from the plane of the disk, with Galactocentric distance  $R_c = 14.0$  kpc, placing it firmly out of the disk and in the Galactic halo. No other isolated neutron stars are known in the halo, although it seems likely that at least some radio pulsars – whose distance estimates make use of the free electron density of the ISM, dominated by the disk component – populate the halo (Manchester et al. 2005). The inferred luminosity of Calvera is then  $L_X$  (0.1–2.4 keV) =  $1.0 \times 10^{34}$  erg s<sup>-1</sup> – an order of magnitude greater than the next most-luminous INS (Fig. 2), due to the high  $kT_{\text{eff}}$  of Calvera.

This location leads to a conundrum. The interstellar medium (ISM) in the halo is too sparse to power Calvera’s X-ray luminosity by accretion. If the source is then powered by remnant heat from the supernova which produced it, then standard cooling curves require a cooling age  $\tau_c < 10^6$  yr old (Page et al. 2006) during which time it must travel at velocity perpendicular to the plane  $v_Z$  a distance of at least  $z = v_Z \tau_c$ ; its distance from the plane then requires  $v_Z > 5100$  km s<sup>-1</sup>, greater than has been previously observed for any NS. Alternatively if the INS is travelling at a more usual  $v_Z = 380$  km s<sup>-1</sup> (Faucher-Giguère & Kaspi 2006), that requires a cooling time of  $\tau_c > 13$  Myr, which cannot be accommodated by either cooling of standard NSs (Page et al. 2004) or of highly magnetized ones (Arras et al. 2004). Thus, the INS hypothesis for Calvera leads to conclusions which challenge existing theory.

While high proper-motion is sometimes used to demonstrate proximity of an astronomical object, one cannot exclude the distant, standard-cooling INS hypothesis with a high proper-motion measurement in this case. This is because a more distant INS (out in the halo) requires a proportionately greater  $v_Z (\geq d \sin(b) / \tau_c)$ . The projection of this velocity across the line of sight results in a distance-independent proper motion  $\mu = \sin(b) \cos(b) / \tau_c$ ; for Calvera, this is  $\mu = 100$  mas yr<sup>-1</sup> for  $\tau_c = 10^6$  yr, independent of Calvera’s distance.

### 3.1.2. Magnetar

While the observation of a slow pulse period,  $P \approx 6$  s, and a rapid spin-down rate (for an AXP identification), or alternatively a burst of gamma-rays (for an SGR identification), would be required to demonstrate a magnetar nature for Calvera, neither possibility can be ruled out with the current set of observations. We thus consider the hypothesis that Calvera is a magnetar.

Recent work has identified a tight clustering of the maximum persistent 2–10 keV X-ray luminosities of magnetars near  $\sim 1.3 \times 10^{35}$  erg s<sup>-1</sup> – making them, in a sense, X-ray standard candles (Woods & Thompson 2006; Durant & van Kerkwijk 2006). Magnetar X-ray spectra (0.1–10 keV) can be described by a soft blackbody ( $kT_{\text{eff}} = 0.41\text{--}0.63$  keV) with a power-law dominating at higher energies (power-law photon index  $\alpha = 2.0\text{--}4.5$ ). While the low signal to noise of our *Swift* XRT spectrum of Calvera does not allow demonstration of multiple spectral components, a single power-law fit across 0.5–10 keV is expected to overestimate the 2–10 keV flux, and hence underestimate the source distance according to this relation. Our best-fit single power-law flux (Table 1), assuming the standard-candle luminosity derived by Durant & van Kerkwijk (2006) for Calvera, yields a distance  $d = 66$  kpc, and a height above the Galactic disk of  $z = 40$  kpc. This would imply an even more extreme space velocity/lifetime (large  $v_Z \tau_c$ ) conundrum than the INS hypothesis considered above.

Alternatively, if (contrary to current evidence) we consider the 2–10 keV luminosity of magnetars to be a free parameter, then we note that known magnetars (Durant & van Kerkwijk 2006; Munro et al. 2006) are all located within  $|z| < 0.1$  kpc of the Galactic plane. Placing Calvera at  $z = +0.1$  kpc, then, yields a distance of  $d < 0.17$  kpc and a 2–10 keV X-ray luminosity  $L_X < 8.7 \times 10^{29}$  erg s<sup>-1</sup>, a factor of  $10^5$  times less luminous than the standard-candle luminosity (Durant & van Kerkwijk 2006) and  $10^3$  times less luminous than the next-faintest known magnetar (Munro et al. 2006).

Calvera, if it is a magnetar, is thus observationally distinguished from all other known magnetars, having either an anomalously small luminosity or an anomalously large Galactic altitude. We thus consider the magnetar hypothesis strongly disfavored.

### 3.1.3. Compact Central Object

The compact central object (CCO) of Cas A (Pavlov et al. 2000) is one of several point-like X-ray sources in the centers of Galactic supernova remnants (SNRs) that have similar spectral properties (Slane et al. 1999; Pavlov et al. 2001; Park et al. 2006). The Cas A CCO is observed with  $kT_{\text{eff}} = 490$  eV and emission radius  $R_{\text{bb}} = 0.29_{-0.09}^{+0.16}$  km at the distance of

Cas A,  $d = 3.4$  kpc. It is unclear why CCOs have apparently smaller  $R_{\text{bb}}$  than magnetars and INs. The small blackbody radii of the CCO sources are inconsistent, in all current theoretical scenarios, with uniform emission from the full surface of a neutron star. A small radius would be expected if these sources emit the majority of their X-ray radiation from hot polar caps covering a fraction of the NS surface; however, the absence of detected pulsations from the CCOs (with the exception of RX J121000.8–522625) casts some doubt on this interpretation. As an alternative, it has been suggested that the CCOs may be accreting black holes.

While the unique class-defining characteristic of a CCO is association with a SNR, and there is no known SNR within 2 deg of Calvera, we may consider the possibility that Calvera is the first “unhosted” CCO.

If we assume a three-dimensional space velocity for Calvera equal to the  $v = 380$  km s<sup>-1</sup> average for radio pulsars (Faucher-Giguère & Kaspi 2006), and an age appropriate to the cooling age for a  $10^6$  K NS,  $\tau = 5 \times 10^5$  yr (Page et al. 2004), then we expect Calvera to have traveled 190 pc from its birthplace. Travelling at a statistical-average angle of 30° with respect to the disk, it would be expected to traverse a vertical distance  $\delta z \approx 95$  pc out of the Galactic plane. Adding this distance to the stellar scale height of the Galactic disk,  $z_* \approx 90$  pc, we expect it to have reached  $z \approx 180$  pc by the time it has cooled to its present temperature. This would then yield a distance  $d = 300$  pc, an emitting radius  $R_{\text{bb}} \approx 0.22$  km, and a luminosity  $L_X = 1.3 \times 10^{31}$  erg s<sup>-1</sup> (0.1–2.4 keV). This would make Calvera a factor of  $\approx 10$  fainter than the faintest known CCO, while giving it a comparable temperature and emitting radius. Such a distance is within reach of a parallax measurement with present instruments (Kaplan et al. 2007).

#### 3.1.4. Millisecond Radio Pulsar

We compare the X-ray properties of Calvera to MSPs observed in the homogeneous survey of the MSP population of 47 Tuc (Bogdanov et al. 2006). Calvera has a similar effective temperature as these MSPs (see Fig. 3); and, for distances between 80 and 260 pc, it has a similar thermal bolometric luminosity ( $10^{30-31}$  erg s<sup>-1</sup>; Fig. 2) and  $R_{\text{bb}}$  (0.06–0.18 km). The <41% r.m.s variability limit is consistent with variability limits on these MSPs (Cameron et al. 2007). Thus, the measured properties of Calvera are consistent with those of an MSP with a distance between 80 and 260 pc.

Intriguingly, one radio pulsar has previously been discovered from a similar X-ray-selected sample (Zepka et al. 1996). If Calvera is a radio pulsar, then, it would not be

unprecedented.

#### 4. Conclusions

We have identified a new isolated compact object at high Galactic latitude ( $b = +37^\circ$ ), Calvera, via its high X-ray to optical flux ratio,  $F_X/F_V > 8700$ .

If Calvera is a typical INS, it would have a distance  $d = 11.1$  kpc which would require a spatial velocity  $v_z > 6700$  km s<sup>-1</sup> to reach this location in less than a cooling time  $\tau_c = 1$  Myr. This velocity is much greater than the  $\approx 380$  km s<sup>-1</sup> value typical to pulsars, and even much greater than the highest directly measured velocity for a neutron star ( $1083_{-90}^{+103}$  km s<sup>-1</sup>, Chatterjee et al. 2005) or the highest implied velocity (800-1600 km s<sup>-1</sup>, Chatterjee & Cordes 2004). Alternatively within the typical INS hypothesis, it would have cooling time ( $\tau_c \geq 17$  Myr) much longer than present cooling-time predictions.

If Calvera is a typical magnetar, its distance would be even greater than in the INS hypothesis, and therefore velocity and cooling-time implications are more disparate from the present observations and theory.

If Calvera is a CCO, it would avoid these velocity and cooling-time implications, but it would be the first such object discovered outside a SNR.

Calvera may be an ICBAS source (“It Can Be Any Size”), which implicitly is not related to any of the known classes, can have any  $R_{bb}$  and thus be at any distance and luminosity (as a function of  $R_{bb}$ ). This hypothesized class of sources is simply a counter-hypothesis to the known classes, making a point of the fact that, in the absence of an assumed  $R_{bb}$  (or, equivalently,  $L_X$ ), we can say nothing about Calvera’s distance or classification.

The only class of objects consistent with the demonstrated properties of Calvera are the radio pulsars; in particular, pulsars analogous to the MSPs observed in the globular cluster 47 Tuc. We therefore conclude that Calvera is most likely a radio pulsar. This could be confirmed by detection of radio pulsations from this source.

If Calvera is a new (perhaps fast) radio pulsar, it would be an observationally useful object. It exhibits an X-ray flux equal to the X-ray-brightest and second closest millisecond radio pulsar, PSR J0437–4715 (Zavlin 2006). There are only 5 known radio pulsars within  $d < 260$  pc, and only one in the northern hemisphere (Manchester et al. 2005)<sup>3</sup>. If Calvera indeed turns out to be an MSP, it would be the third closest MSP in the sky (after PSR J0437-

---

<sup>3</sup><http://www.atnf.csiro.au/research/pulsar/psrcat>

4715 at  $d = 160$  pc and PSR J2124-3358 and  $d = 250$  pc) and potentially the closest MSP at  $d = 80$  pc. It would be the closest MSP in the northern hemisphere (followed by PSR J0030+0451,  $d=300$  pc) making it a potentially useful target both for a pulsar timing array (Foster & Backer 1990) and for targeted search with the *Laser Interferometric Gravitational Wave Observatory* (LIGO; e.g. Cutler 2002).

We would like to express our gratitude to the *Swift* operations team for the fill-in target observations that made this work possible. We gratefully acknowledge Jean-Rene Roy for granting director's discretionary time with Gemini-North for this project. We are also grateful to Harvey Tananbaum for granting director's discretionary time with *Chandra* for this project. We gratefully acknowledge and thank the anonymous referee, for suggestions regarding the SWIFT data analysis which corrected an earlier version, changing the quantitative conclusions. RER gratefully acknowledges useful conversations with A. Cumming, an advocate of the strong ICBAS hypothesis. RER is supported by the Natural Sciences and Engineering Research Council of Canada Discovery program.

## REFERENCES

- Arnaud, K. A. 1996, in *Astronomical Data Analysis Software and Systems V.*, ed. G. Jacoby & J. Barnes, Vol. 101 (ASP Conf. Series), 17
- Arras, P., Cumming, A., & Thompson, C. 2004, *ApJ*, 608, L49
- Bogdanov, S., Grindlay, J. E., Heinke, C. O., Camilo, F., Freire, P. C. C., & Becker, W. 2006, *ApJ*, 646, 1104
- Burrows, D. N. et al. 2003, in *X-Ray and Gamma-Ray Telescopes and Instruments for Astronomy*. Edited by Joachim E. Truemper, Harvey D. Tananbaum. Proceedings of the SPIE, Volume 4851, 1320
- Burwitz, V., Haberl, F., Neuhäuser, R., Predehl, P., Trümper, J., & Zavlin, V. E. 2003, *A&A*, 399, 1109
- Cameron, P. B., Rutledge, R. E., Camilo, F., Bildsten, L., Ransom, S. M., & Kulkarni, S. R. 2007, *ApJ*, 660, 587
- Carter, C., Karovska, M., Jerius, D., Glotfelty, K., & Beikman, S. 2003, in *Astronomical Society of the Pacific Conference Series*, Vol. 295, *Astronomical Data Analysis Software and Systems XII*, ed. H. E. Payne, R. I. Jedrzejewski, & R. N. Hook, 477–+

- Cash, W. 1979, *ApJ*, 228, 939
- Chatterjee, S. & Cordes, J. M. 2004, *ApJ*, 600, L51
- Chatterjee, S. et al. 2005, *ApJ*, 630, L61
- Cutler, C. 2002, *Phys. Rev. D*, 66, 084025
- Dickey, J. M. & Lockman, F. J. 1990, *ARA&A*, 28, 215
- Durant, M. & van Kerkwijk, M. H. 2006, *ApJ*, 650, 1070
- Faucher-Giguère, C.-A. & Kaspi, V. M. 2006, *ApJ*, 643, 332
- Foster, R. S. & Backer, D. C. 1990, *ApJ*, 361, 300
- Fox, D. B. 2004, *ArXiv Astrophysics e-prints*, astro-ph/0403261
- Fruscione, A. et al. 2006, in Presented at the Society of Photo-Optical Instrumentation Engineers (SPIE) Conference, Vol. 6270, *Observatory Operations: Strategies, Processes, and Systems*. Edited by Silva, David R.; Doxsey, Rodger E.. Proceedings of the SPIE, Volume 6270, pp. 62701V (2006).
- Gehrels, N. et al. 2004, *ApJ*, 611, 1005
- Haberl, F. 2005, in 5 years of Science with XMM-Newton, ed. U. G. Briel, S. Sembay, & A. Read, 39
- Haberl, F. 2006, *ArXiv.org*, astro-ph/0609066, 1
- Haberl, F., Motch, C., Buckley, D. A. H., Zickgraf, F. J., & Pietsch, W. 1997, *A&A*, 326, 662
- Haberl, F. et al. 2004, *A&A*, 424, 635
- Haberl, F., Turolla, R., de Vries, C. P., Zane, S., Vink, J., Méndez, M., & Verbunt, F. 2006, *A&A*, 451, L17
- Ho, W. C. G., Kaplan, D. L., Chang, P., van Adelsberg, M., & Potekhin, A. Y. 2007, *MNRAS*, 375, 821
- Hui, C. Y. & Becker, W. 2006, *A&A*, 454, 543
- Kaplan, D. L., van Kerkwijk, M. H., & Anderson, J. 2002, *ApJ*, 571, 447

- 2007, ArXiv Astrophysics e-prints, astro-ph/0703343
- Lattimer, J. M. & Prakash, M. 2004, *Science*, 304, 536
- Manchester, R. N., Hobbs, G. B., Teoh, A., & Hobbs, M. 2005, *AJ*, 129, 1993
- Monet, D. G. et al. 2003, *AJ*, 125, 984
- Motch, C., Haberl, F., Zickgraf, F.-J., Hasinger, G., & Schwope, A. D. 1999, *A&A*, 351, 177
- Muno, M. P. et al. 2006, *ApJ*, 636, L41
- Muno, M. P., Gaensler, B. M., Clark, J. S., de Grijs, R., Pooley, D., Stevens, I. R., & Portegies Zwart, S. F. 2007, *MNRAS*, 378, 44
- Murray, S. S., Chappell, J. H., Kenter, A. T., Kraft, R. P., Meehan, G. R., & Zombeck, M. V. 1998, in *Proc. SPIE Vol. 3356*, p. 974-984, *Space Telescopes and Instruments V*, Pierre Y. Bely; James B. Breckinridge; Eds., Vol. 3356, 974
- Page, D., Geppert, U., & Weber, F. 2006, *Nuclear Physics A*, 777, 497
- Page, D., Lattimer, J. M., Prakash, M., & Steiner, A. W. 2004, *ApJS*, 155, 623
- Page, D. & Reddy, S. 2006, Arxiv.org, astro-ph/0608360, *annu. Rev. Nucl. & Part. Sci.*, in press
- Park, S., Mori, K., Kargaltsev, O., Slane, P. O., Hughes, J. P., Burrows, D. N., Garmire, G. P., & Pavlov, G. G. 2006, *ApJ*, 653, L37
- Pavlov, G. G., Sanwal, D., Kızıltan, B., & Garmire, G. P. 2001, *ApJ*, 559, L131
- Pavlov, G. G., Zavlin, V. E., Aschenbach, B., Trümper, J., & Sanwal, D. 2000, *ApJ*, 531, L53
- Pons, J. A., Walter, F. M., Lattimer, J. M., Prakash, M., Neuhäuser, R., & An, P. 2002, *ApJ*, 564, 981
- Roming, P. W. et al. 2000, in *Proc. SPIE Vol. 4140*, p. 76-86, *X-Ray and Gamma-Ray Instrumentation for Astronomy XI*, Kathryn A. Flanagan; Oswald H. Siegmund; Eds., 76
- Rutledge, R. E., Brunner, R. J., Prince, T. A., & Lonsdale, C. 2000, *ApJS*, 131, 335
- Rutledge, R. E., Fox, D. W., Bogosavljevic, M., & Mahabal, A. 2003, *ApJ*, 598, 458

- Schwope, A. D., Hasinger, G., Schwarz, R., Haberl, F., & Schmidt, M. 1999, *A&A*, 341, L51
- Slane, P., Gaensler, B. M., Dame, T. M., Hughes, J. P., Plucinsky, P. P., & Green, A. 1999, *ApJ*, 525, 357
- Taylor, J. H. & Cordes, J. M. 1993, *ApJ*, 411, 674
- Voges, W. et al. 1999, *A&A*, 349, 389
- Walter, F. M. & Lattimer, J. M. 2002, *ApJ*, 576, L145
- Walter, F. M. & Matthews, L. D. 1997, *Nature*, 389, 358
- Walter, F. M., Wolk, S. J., & Neuhauser, R. 1996, *Nature*, 379, 233
- Woods, P. M. & Thompson, C. 2006, Soft gamma repeaters and anomalous X-ray pulsars: magnetar candidates (Compact stellar X-ray sources), 547–586
- Zampieri, L., Campana, S., Turolla, R., Chierigato, M., Falomo, R., Fugazza, D., Moretti, A., & Treves, A. 2001, *A&A*, 378, L5
- Zavlin, V. E. 2006, *ApJ*, 638, 951
- Zepka, A., Cordes, J. M., Wasserman, I., & Lundgren, S. C. 1996, *ApJ*, 456, 305

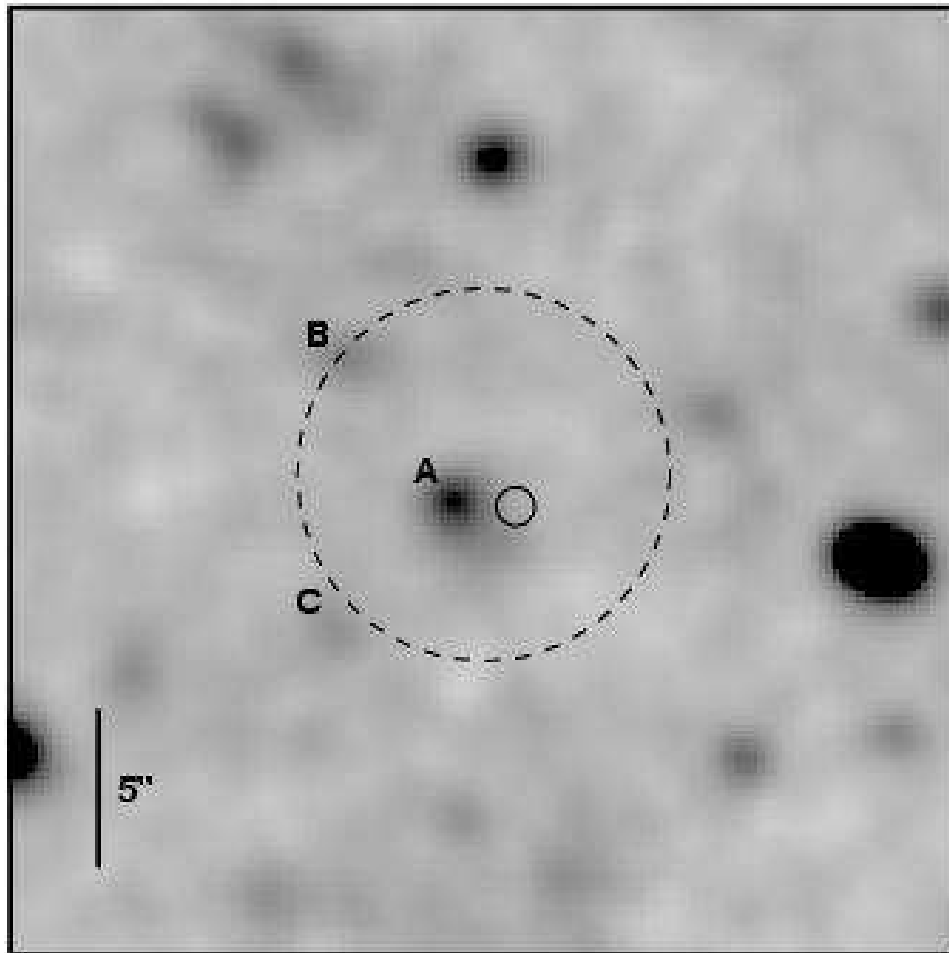


Fig. 1.— Gemini North + GMOS  $g$ -band image of the 90%-confidence X-ray (*Chandra* HRC-I) localization for Calvera (solid circle, radius  $0.57''$ ), showing the absence of an optical counterpart to deep limits; the dashed circle (radius  $5.9''$ ) indicates the 90%-confidence *Swift* XRT localization. Our three-sigma limit over the *Chandra* localization is  $g > 26.3$  mag, giving  $F_X/F_V > 8700$  after accounting for extinction. The image is smoothed with a PSF-like Gaussian kernel of FWHM  $1.2''$  to reveal faint sources, three of which (A–C) are consistent with the *Swift* localization. North is up, East is to the left, and the image scale is indicated. The nearest point source (“A”), southeast of *Chandra* localization, has  $g = 24.8$  mag and is excluded as a counterpart with  $> 3.8\sigma$  confidence.

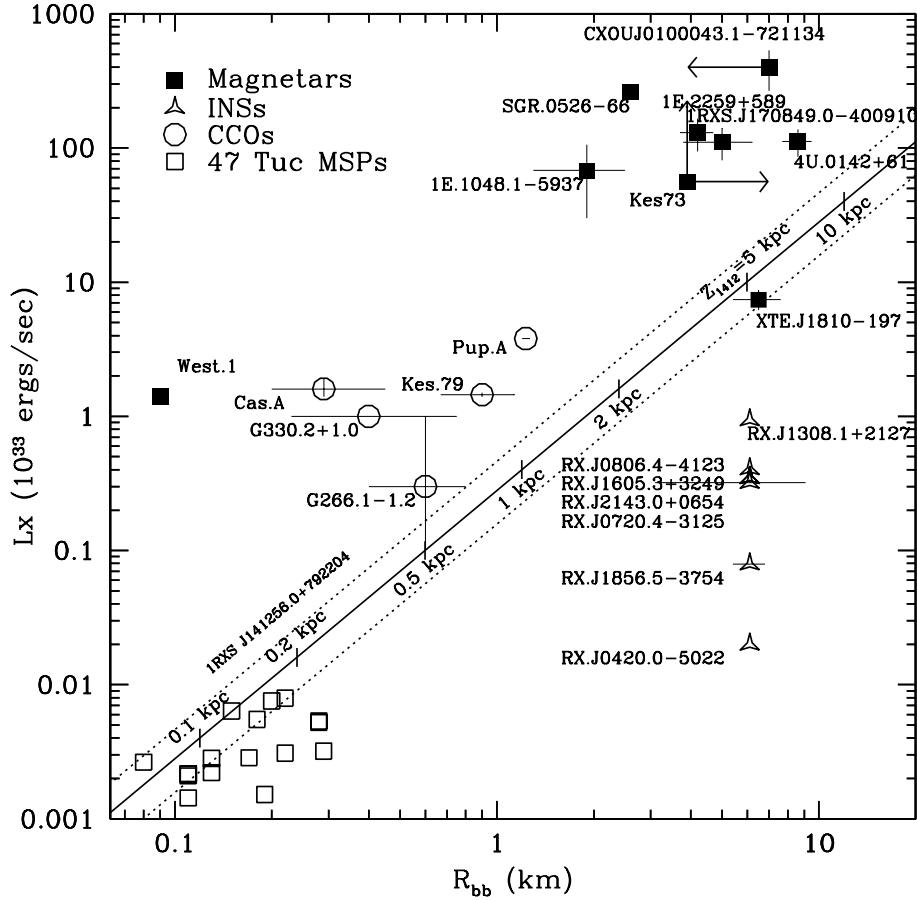


Fig. 2.— The blackbody radius  $R_{\text{bb}}$  and  $L_X$  values for magnetars (solid squares), CCOs (open circles), INSs (3-pointed stars), and MSPs in 47 Tuc (open squares). The distances of the INSs have been normalized to the parallax distance of 1RXS J185635.1–375433, assuming all have the same  $R_{\text{bb}}$ ; see Table 2 and text for details. The solid line indicates the best-fit  $R_{\text{bb}}$  vs.  $L_x$ , hash-marked with the  $z$  for Calvera; the dotted-lines contain the 90% uncertainty in  $R_{\text{bb}}$  for Calvera. Interpreting Calvera as an INS implies that it lies a vertical distance  $z = 5.1$  kpc above the Galactic disk, at a Galactocentric distance of  $R_c = 14.0$  kpc, well outside the disk and in the Galactic halo. Interpreting Calvera as a persistent magnetar leads to a paradox, since all other magnetars are found within a vertical distance  $|z| < 0.1$  kpc of the disk, yet a large  $z$  is required for Calvera to have a luminosity ( $L_X \approx 10^{35}$  erg s $^{-1}$ ) appropriate to the population. Even with a luminosity as low as that of the transient magnetar, XTE J1810-197,  $z > 4.9$  kpc is required. Interpreting Calvera as a CCO – despite the absence of any surrounding supernova remnant – implies that it is either the faintest member of this population, or lies at a vertical distance  $z \approx 1$  to 5 kpc above the disk. Calvera has  $L_x$  and  $R_{\text{bb}}$  consistent with those of the radio MSPs in 47 Tuc, if its distance is in the range 80-260 pc.

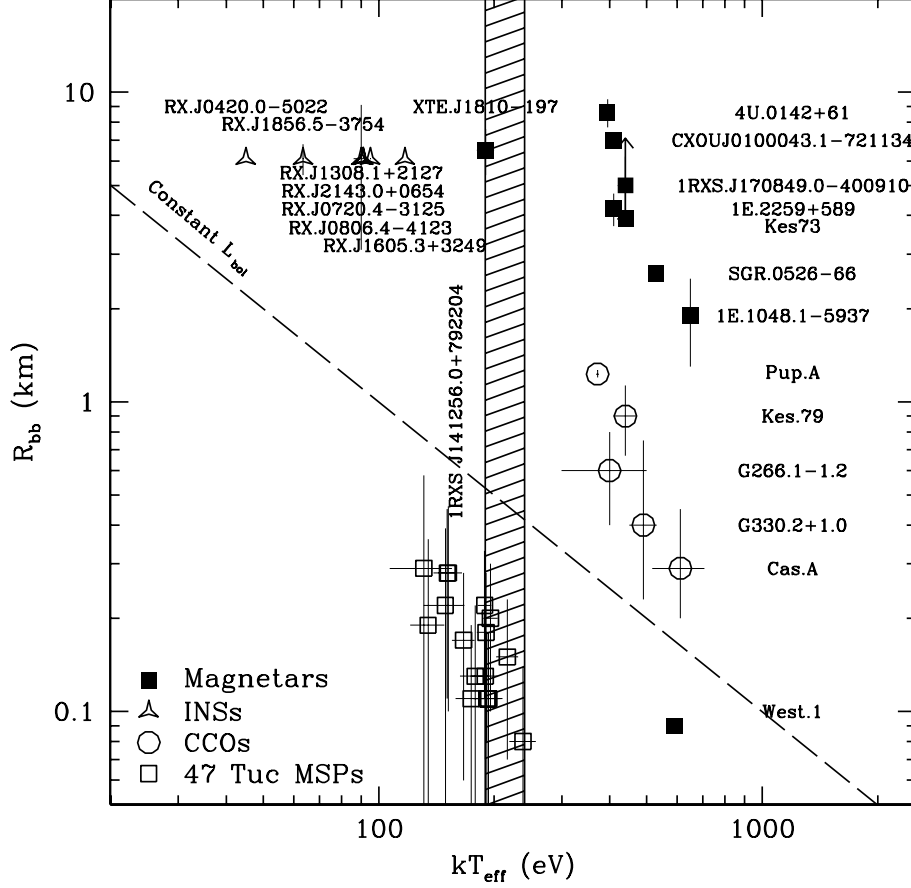


Fig. 3.— The effective temperature  $kT_{\text{eff}}$  and blackbody radius  $R_{\text{bb}}$  for magnetars, CCOs, INSs, and MSPs in 47 Tuc (see Fig. 2 and text for discussion). The hashed region indicates the  $kT_{\text{eff}}$  value for Calvera; it covers all values of  $R_{\text{bb}}$  due to the unknown distance. It overlaps  $kT_{\text{eff}}$  for the 47 Tuc MSPs, if Calvera is within a distance range of roughly 80 to 260 pc.

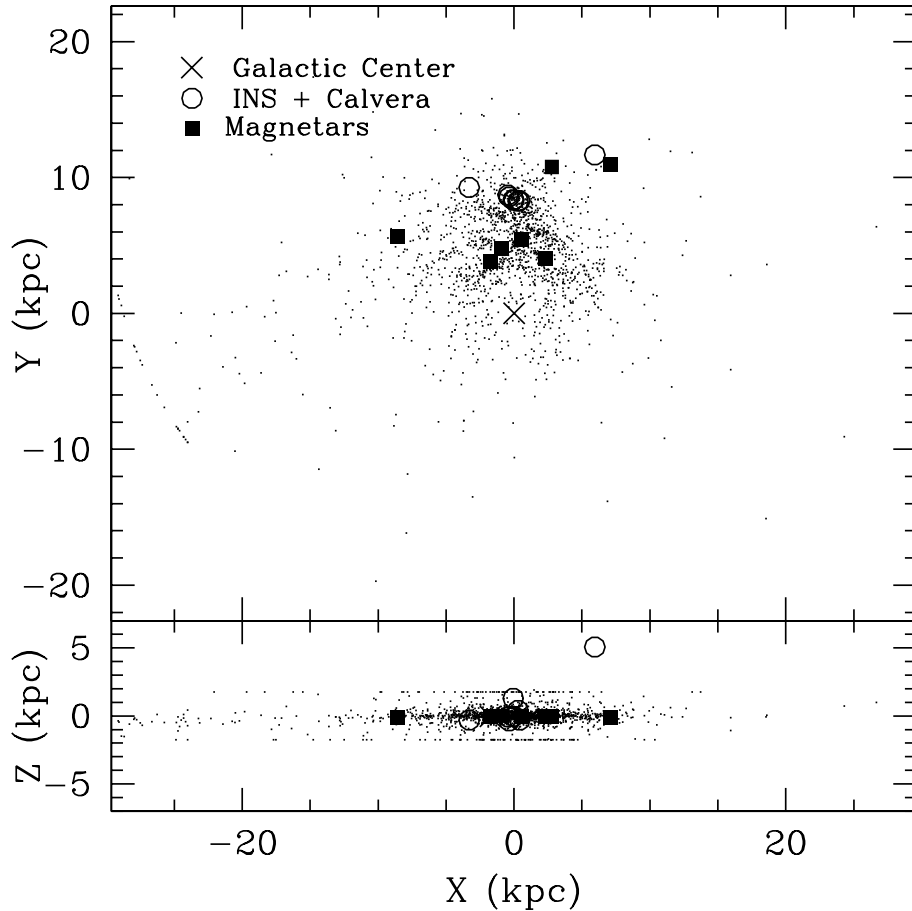


Fig. 4.— The galactic distribution of radio pulsars in the ATNF pulsar catalog (black points; Manchester et al. 2005) – with objects associated with globular clusters and known extragalactic sources removed – magnetars (solid squares; distances from Durant & van Kerkwijk 2006; Muno et al. 2006), and INSs and Calvera (assuming INSs and Calvera have the same  $R_{bb}$ ; open circles, from Table 2). The implication of interpreting all INSs as having the same  $R_{bb}$  is that they are a spatially homogeneous population – local, within the disk of the galaxy. However, including Calvera in this class places it well above the Galactic disk (bottom panel) at  $z \approx 5.1$  kpc.

Table 1. Characteristics of Calvera

Characteristic	Value
Right Ascension (J2000)	14 <sup>h</sup> 12 <sup>m</sup> 55 <sup>s</sup> .885
Declination (J2000)	+79°22′04″.10
Uncertainty radius (90%)	0.57″
UVOT Limit	$f_{\text{UVM}2} < 1.3 \times 10^{-17} \text{ erg cm}^{-2} \text{ s}^{-1}$
Gemini Limit ( $3\sigma$ )	$g > 26.3 \text{ mag}$
Blackbody Energy Spectrum	
$kT_{\text{eff}}$	215±25 eV
Normalization	$7.2_{-1.8}^{+2.4} (R_{\text{km}}/D_{10\text{kpc}})$
Corrected X-ray Flux	$1.2 \times 10^{-12} \text{ (erg cm}^{-2} \text{ s}^{-1}; 0.1\text{--}2.4 \text{ keV)}$
$N_H$ (fixed)	$3 \times 10^{20} \text{ cm}^{-2}$
C-statistic	23.97
Power Law Energy Spectrum	
Photon Slope $\alpha$	2.8±0.3
Corrected X-ray Flux	$2.5 \times 10^{-13} \text{ (erg cm}^{-2} \text{ s}^{-1}; 2\text{--}10 \text{ keV)}$
$N_H$ (fixed)	$3 \times 10^{20} \text{ cm}^{-2}$
C-statistic	30.03

Note. — Properties of the isolated neutron star Calvera (1RXS J141256.0+792204). Parameters are estimated using the X-ray spectral modelling package XSPEC v12.3.0 (Arnaud 1996). The X-ray equivalent hydrogen column density was fixed at the value of the integrated column through the galaxy in the direction of the source (Dickey & Lockman 1990). Uncertainties are quoted at 90% confidence. X-ray fluxes are corrected for interstellar absorption. Blackbody and power-law spectral parameters are independently derived by fitting to the same *Swift* XRT data, over 0.5–10 keV.

Table 2. Galacto-centric Positions of INSS and Calvera in an INS Interpretation

Source	$kT_{\text{eff}}$ (eV)	$F_X$	(l,b) (deg,deg)	$X$ (kpc)	$Y$ (kpc)	$Z$ (kpc)	$d$ (kpc)	$R_c$ (kpc)	Refs.
1RXS J0420.0–5022	45	5	258, -44	-0.36	8.58	-0.35	0.51	8.59	1
RXJ0720.4–3125	90	100	244, -8	-0.45	8.72	-0.07	0.50	8.73	2
RXJ0806.4–4123	95	2.8	257, -5	-3.29	9.26	-0.30	3.39	9.83	3
1RXS J130848.6+212708	117	45	339, 83	-0.06	8.35	1.29	1.30	8.45	4
Calvera	215	12	118, 37	5.9	11.66	5.08	8.43	14.04	present
1RXS J1605.3+3249	91	88	53, 48	0.30	8.27	0.42	0.56	8.29	5
1RXS J185635.1–375433	63.5	210	359, -17	0.00	8.34	-0.05	0.167	8.34	6
1RXS J214303.7+065419	91	87	63, -33	0.42	8.29	-0.31	0.56	8.30	7

Note. — Galactic positions of the seven INSSs, plus Calvera, under the assumption all have the same  $R_{\text{bb}}$  as 1RXS J185635.1–375433 at a distance of 167 pc (see text). Reading across the columns, we give the source name, the measured effective temperature, the X-ray flux in units of  $10^{-13}$  erg cm $^{-2}$  s $^{-1}$  (0.1 – 2.4 keV); the galactic longitude and latitude (l,b); the resulting galactic three dimensional coordinates  $X$ ,  $Y$ , and  $Z$ , where (0,0,0) is Galactic Center, and (0,8.5,0) is the Sun’s location (Taylor & Cordes 1993); the source’s distance from the Sun  $d$ ; and galacto-centric distance  $R_c$ , with the relevant references. These positions are plotted in Fig. 4.

References. — 1, Haberl et al. (2004); 2, Haberl et al. (2006); 3, Haberl et al. (2004); 4, Schwope et al. (1999); 5, Motch et al. (1999); 6, Burwitz et al. (2003); Kaplan et al. (2007); 7, Zampieri et al. (2001)